

# Electrically Programmable Equivalent-Phase-Shifted Waveguide Bragg Grating for Multichannel Signal Processing

Weifeng Zhang and Jianping Yao

*Microwave Photonics Research Laboratory, School of Electrical Engineering and Computer Science,  
University of Ottawa, 800 King Edward Avenue, Ottawa, Ontario, Canada K1N 6N5  
jpyao@eecs.uottawa.ca*

**Abstract:** A silicon-based on-chip electrically programmable equivalent-phase-shifted waveguide Bragg grating implemented through nonuniform spatial sampling to introduce an equivalent phase shift is designed, fabricated and characterized, and its application in multichannel signal processing is experimentally demonstrated. © 2019 The Author(s)  
**OCIS codes:** (130.3120) Integrated optics devices; (050.2770) Gratings;

## 1. Introduction

Since the discovery of fiber Bragg gratings (FBGs) by Hill and co-workers in 1978, FBGs have played a key role in the fields of telecommunications and optical sensing. With the rapid development of photonic integrated circuits (PICs), on-chip waveguide Bragg gratings have been extensively researched [1, 2]. In particular, thanks to the compatibility with the mature CMOS fabrication process and potential for seamless integration with electronics, great efforts have been directed to the study of using silicon as a photonic integration material system [3]. Recently, a fully reconfigurable waveguide Bragg grating on a silicon photonic chip is reported [4]. By incorporating multiple PN junctions, the entire index modulation profile of the grating could be electrically reconfigured by field programming all the bias voltages, which enables the grating to have diverse spectral characteristics for diverse applications. The key to implement this reconfigurable grating is to introduce an accurate phase shift. However, due to the poor fabrication tolerance of the currently available silicon fabrication process, the phase shift is not accurate which imposes a major limitation on the spectral accuracy of a phase-shifted Bragg grating. To make a grating have a precise spectral response without using high-precision lithography, a solution is to use the equivalent phase shift (EPS) technique [5].

In this paper, we report the design, fabrication, and experimental demonstration of a silicon-based on-chip electrically programmable EPS waveguide Bragg grating. By incorporating the programmable grating in a microwave photonic system, a multichannel signal processor is experimentally demonstrated.

## 2. Design and Measurement

Fig. 1(a) illustrates the schematic of a programmable EPS waveguide Bragg grating on a silicon photonic chip. The grating is produced by creating periodic corrugations on the waveguide sidewalls, which is shown in the inset of Fig. 1(a). Fig. 1(b) gives a zoom-in view of the EPS Bragg grating. An equivalent phase shift is realized by spatially sampling a uniform grating to create an increased sampling period  $P + \Delta L$  in the center of the grating, where  $P$  is spatial sampling period and  $\Delta L$  is the sampling period increment. Based on the EPS principle, if a uniform grating with a grating pitch  $\Lambda$  is spatially sampled with a spatial sampling function having a sampling period  $P$ , where  $P \gg \Lambda$ , a multiple channel transmission spectrum would be produced. In our design, the sampling period increment is selected to be  $\Delta L = P/2$ , which leads to an odd integer number of  $\pi$  phase shift to the odd-order channels. Considering the sampling period  $P$  is three orders of magnitude larger than the grating pitch  $\Lambda$ , the requirement for lithography accuracy would be highly reduced, compared to the implementation of a conventional phase-shifted grating in which a phase shift block with a length of  $\Lambda/2$  is added.

To make the grating electrically programmable, independent lateral PN junctions are incorporated along the grating. As shown in Fig. 1(b), in a sampling period, two independent PN junctions are distributed in the on-modulation grating section and off-modulation grating section. To avoid mutual electrical coupling between neighboring PN junctions, a section of undoped waveguide is used as an electrical insulator. Fig. 1(c) shows the cross-sectional view of the lateral PN junction along the dashed line AA' in Fig. 1(b). Since the free-carrier plasma dispersion effect is more sensitive to the change of the free-hole concentration, to achieve a higher tuning efficiency, an asymmetrical lateral PN junction is used by slightly shifting the junction center of 50 nm to the left from the waveguide center. Fig. 1(d) gives the top-view of the proposed EPS Bragg grating. In our design, the entire device has 11 sampling periods in total. Fig. 1(e) is a photograph of the input grating coupler of the fabricated grating. Fig. 1(f) gives a photograph of one sampling period of the EPS Bragg grating. The grating pitch  $\Lambda$  is 310 nm with a duty cycle of 50%, and the periodic sidewall corrugation has a depth as large as 100 nm, which makes the grating work in the C band. The spatial sampling period is 255.75  $\mu\text{m}$  including a 7.75- $\mu\text{m}$ -long undoped waveguide for electrical insulation. Fig. 1(g) provides a photograph of the increased sampling period in the center of the EPS Bragg grating. The

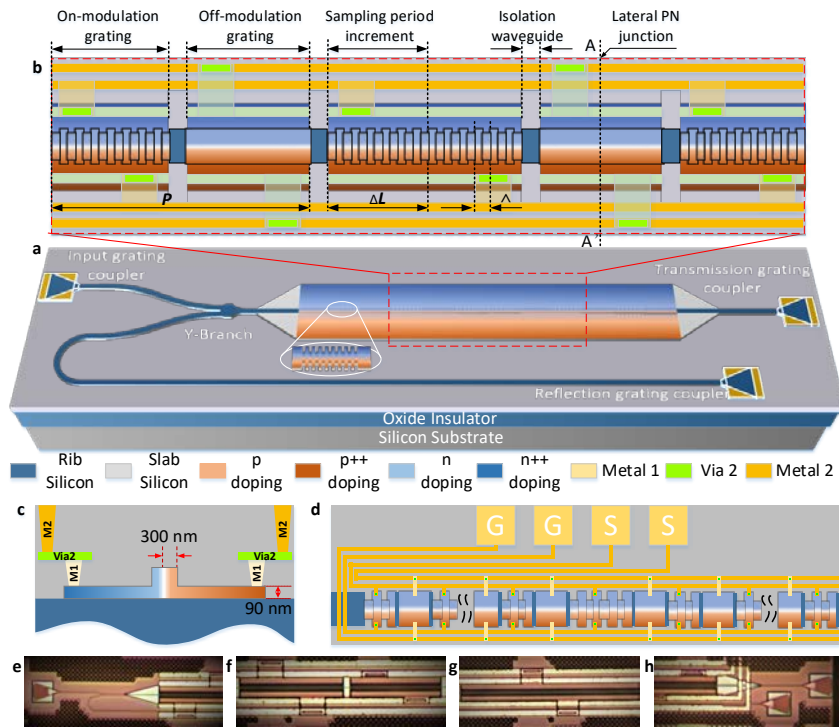


Fig. 1. (a) Perspective view of the proposed programmable EPS waveguide Bragg grating on a silicon photonic chip; (b) zoom-in view of the grating structure; (c) cross-sectional view of the waveguide with doping in the grating; (d) top-view of the designed EPS Bragg grating; (e) photograph of the input grating coupler; (f) photograph of a sampling period in the fabricated grating; (g) photograph of the increased sampling period  $\Delta L$ ; and (h) photograph of transmission and reflection grating couplers.

the odd-order channels, a passband in the transmission stopband and a notch in the reflection passband are observed, which are the typical spectral features of a phase-shifted Bragg grating and confirms the effectiveness of the EPS approach in the implementation of a phase-shifted Bragg grating. Fig. 2(b) shows a zoom-in view of the reflection and transmission spectra of the negative-order channels. As can be seen, only the odd-order channels have EPS-resulted spectral features, while the even-order channels have spectral responses that are not affected by the EPS. This is understandable because all even-order channels will have a phase shift that is an integer number of  $2\pi$ . The channel space is calculated to be 1.2 nm, which matches well with the theoretical calculation. Thanks to the strong index modulation of the waveguide grating, the 11<sup>th</sup> channel spectral response could still be seen. Fig. 2(c) shows the reflection and transmission spectra of the positive order channels. The spectral responses of the odd-order channels with EPS-resulted spectral features are clearly seen, while the spectral responses of the even-order channels disappear, which is due to

sampling period increment  $\Delta L$  is chosen to be 124  $\mu\text{m}$  for an odd integer number of  $\pi$  phase shift in the odd-order channels. Fig. 1(h) gives a photograph of the transmission and reflection grating couplers. The entire device has a length of 3.2 mm and a width of 0.25 mm in total, giving a small footprint of 0.8  $\text{mm}^2$ . The key advantages of the programmable ESP Bragg grating include largely reduced requirements for fabrication accuracy and the availability of phase shift tuning via electrically tuning the distributed PN junctions.

Fig. 2(a) shows the measured reflection and transmission spectra of the fabricated EPS Bragg grating in the static state. The red line shows the measured transmission spectrum, while the blue line shows the measured reflection spectrum. Thanks to the spatial sampling, the grating has a multichannel reflection and transmission spectra. Due to the equivalent phase shift caused by the increased sampling period, in

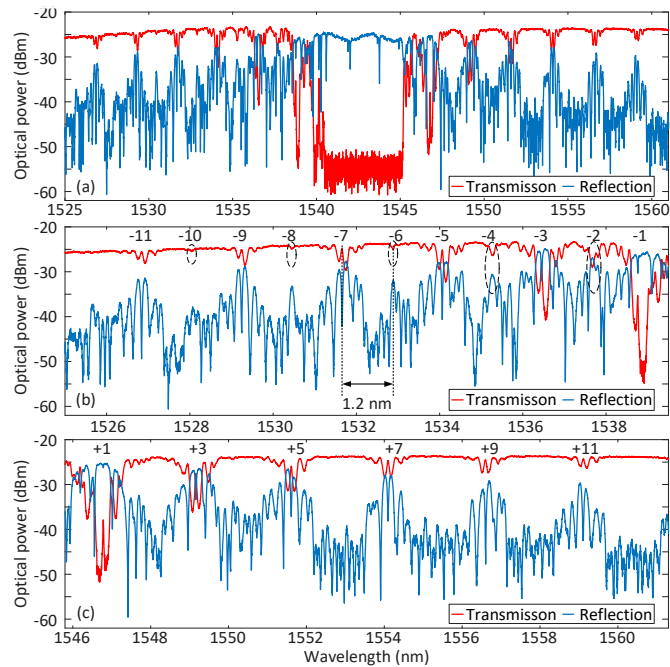


Fig. 2. (a) Measured reflection and transmission spectra of the fabricated EPS Bragg grating; (b) zoom-in view of the negative-order channels spectra; and (c) zoom-in view of the positive-order channels spectra.

the coupling of the even-order modes into the cladding.

Fig. 3(a) shows the measured reflection and transmission spectra of the +3<sup>rd</sup> channel in the static state. A passband is produced in the stopband in the transmission spectrum and a notch is produced in the passband of the reflection spectrum.

The notch in the reflection band has a 3-dB bandwidth of 28 pm. The Q-factor is calculated to be 55,300 and the extinction ratio is 6.4 dB. When the two bias voltages are simultaneously and synchronously changed from -19 to +1 V, the grating spectrum would be shifted. Fig. 3(b) shows the measured transmission spectra of the grating. For the PN junctions being reverse biased, the spectrum is red shifted; while, for the PN junctions being forward biased, the spectrum is blue shifted. Fig. 3(c) shows the tuning of the extinction ratio while the notch wavelength is maintained unchanged for different bias voltage combinations. It is known that in a conventional phase-shifted Bragg grating, it is not possible to tune the extinction ratio while maintaining the notch wavelength unchanged. In the fabricated grating, by field programming the bias voltages, the notch wavelength shifts induced by the on- and off-modulation grating sections can counteract. Thus, the notch wavelength can be kept unchanged, while different bias voltage combinations could lead to a different loss, which leads to a different extinction ratio. The extinction ratio is changed from 6.4 to 4.5 dB. Fig. 3(d) shows the phase response of the reflection notch in the +3<sup>rd</sup> channel, in which the phase jump at the notch center can be tuned from 1.0 to 0.48. The tuning range could be increased by independently controlling the PN junction of the increased sampling period.

### 3. Multichannel differentiation demonstration

As a distinct feature of an EPS Bragg grating is that multichannel phase shifts can be introduced, which is of help for simultaneous manipulation of multiple wavelengths, thus increasing the capability of the grating for programmable multichannel signal processing. A multichannel temporal differentiator with a channel spacing of 2.4 nm is experimentally demonstrated. Fig. 4 shows the measured temporally differentiated pulses at the output of the grating for an input Gaussian pulse, which confirms the effectiveness of the use of the grating to perform multichannel fractional-order differentiation.

### 4. Conclusion

A silicon-based on-chip electrically programmable EPS waveguide Bragg grating was designed, fabricated and experimental demonstrated. By incorporating the programmable EPS grating in a microwave photonic system, a multichannel microwave photonic differentiator was experimentally demonstrated.

### 5. References

- [1] X. Wang, W. Shi, H. Yun, S. Grist, N. A. F. Jaeger, and L. Chrostowski, *Opt. Express* **20**, 15547–15558 (2012).
- [2] H. C. Kim, K. Ikeda, and Y. Fainman, *J. Lightw. Technol.* **25**, 1147–1151 (2007).
- [3] M. Hochberg and T. Baehr-Jones, *Nat. Photon.* **4**, 492–494 (2010).
- [4] W. Zhang and J. P. Yao, *Nature Comm.*, **9**, 1396 (2018).
- [5] Y. Dai, X. Chen, D. Jiang, S. Xie, and C. Fan, *IEEE Photon. Technol. Lett.* **16**, 2284–2286 (2004).

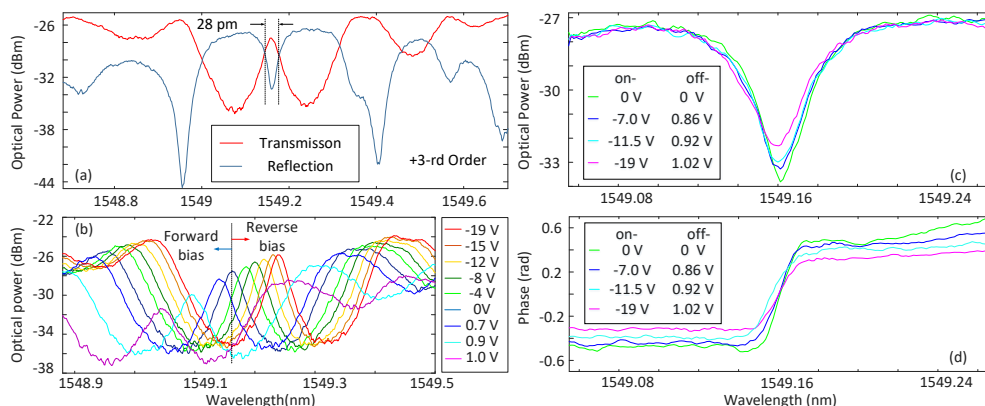


Fig. 3 (a) Measured reflection and transmission spectra of the +3<sup>rd</sup> channel in the static state; (b) measured transmission spectrum of the +3<sup>rd</sup> channel when two bias voltages are synchronously sweeping; (c) tuning of the extinction ratio of the reflection notch in the +3<sup>rd</sup> channel with the notch wavelength kept unchanged, and (d) tuning of the phase jump of the reflection notch in the +3<sup>rd</sup> channel.

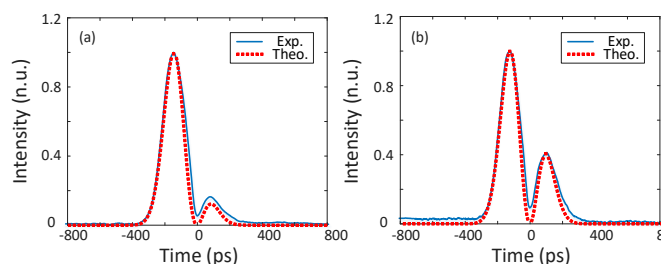


Fig. 4. Differentiated pulses corresponding to a differentiation order of (a)  $n = 0.53$  at the +5<sup>th</sup> channel, and (b)  $n = 0.74$  at the 7<sup>th</sup> channel.